Liquid Crystals
Publication details, including instructions for authors and subscription information:
http://www.informaworld.com/smpp/title~content=t713926090

Effect of lateral substitution on supramolecular liquid crystal associates induced by hydrogen-bonding interactions between 4-(4'-pyridylazo-3-methylphenyl)-4''-alkoxy benzoates and 4-substituted benzoic acids

Magdi M. Naoum[a]; Abdelgawad A. Fahmi[a]; Sayed Z. Mohammady[a]; Amira H. Abaza[a]
[a] Department of Chemistry, Faculty of Science, Cairo University, Cairo, Egypt

To cite this Article Naoum, Magdi M. , Fahmi, Abdelgawad A. , Mohammady, Sayed Z. and Abaza, Amira H.(2010) 'Effect of lateral substitution on supramolecular liquid crystal associates induced by hydrogen-bonding interactions between 4-(4'-pyridylazo-3-methylphenyl)-4''-alkoxy benzoates and 4-substituted benzoic acids', Liquid Crystals, 37: 4, 475 — 486

To link to this Article: DOI: 10.1080/02678291003681378

URL: http://dx.doi.org/10.1080/02678291003681378

Liquid Crystals,
Vol. 37, No. 4, April 2010, 475–486

Effect of lateral substitution on supramolecular liquid crystal associates induced by hydrogen-bonding interactions between 4-(4′-pyridylazo-3-methylphenyl)-4″-alkoxy benzoates and 4-substituted benzoic acids

Magdi M. Naoum*, Abdelgawad A. Fahmi, Sayed Z. Mohammady and Amira H. Abaza

Department of Chemistry, Faculty of Science, Cairo University, Cairo, Egypt

(Received 21 November 2009; final version received 5 February 2010)

Five laterally methyl-substituted pyridine-based derivatives of the title compounds (**I***8*–**I***16*), with molecular formula 4-$C_nH_{2n+1}O$-$C_6H_4COOC_6H_3(3\text{-}CH_3)$-N=N-$C_5H_4N$ were prepared and their molecular formulae elucidated via elemental analyses, infrared, nuclear magnetic resonance and mass spectra. The number of carbon atoms in the alkoxy chain (*n*) varies between 8, 10, 12, 14, and 16 carbons. The newly prepared pyridine-based derivatives were investigated for their mesophase behaviour by differential scanning calorimetry and polarised optical microscopy; most of them were found to possess monotropic smectic C (SmC) mesophase. Two groups (**A** and **B**) of the 1:1 hydrogen-bonded associates, formed between each of the derivatives **I***8*–**I***16* and two types of 4-substituted benzoic acids (**II**), were prepared and similarly characterised to investigate the effect of lateral methyl substitution on the central phenylene ring, as well as terminal polar substituents and alkoxy-chain length on the stability of the mesophases induced by intermolecular hydrogen bonding. In Group **A** complexes, mesomorphic 4-alkoxy benzoic acids, that carry the terminal *n*-alkoxy group of varying chain length, were used. The other series of complexes (Group **B**) is composed from the same pyridine-based derivatives and each of the non-mesomorphic 4-substituted benzoic acids that carries small compact polar groups, varying between CH_3O, CH_3, H, Cl, Br, and CN. All complexes prepared were investigated for their mesophase behaviour by differential scanning calorimetry and polarised optical microscopy and found to be purely smectogenic, possessing SmC as the only mesophase observed. The formation of the hydrogen-bonded complexes was confirmed by constructing their binary phase diagrams, which cover the whole range of concentration of the two complements.

Keywords: supramolecular LCs; 4-(4′-pyridylazo-3-methylphenyl)-4″-alkoxy benzoates; 4-substituted benzoic acids

1. Introduction

The preparation and mesophase behaviour of supramolecular liquid crystals, obtained via hydrogen-bonding interaction between complementary molecules, have been extensively studied in the last 15 years [1–10]. For the formation of a mesomorphic material through hydrogen bonding, complementarity of the interacting molecules constitutes a major factor that contributes to the exhibition of liquid crystallinity. The shape and stability of the hydrogen-bonded complexes are also essential. The first example of a liquid crystal formed via hydrogen bond interaction between carboxyl and pyridyl moieties was reported by Kato and Frechet [11] in 1989. A supramolecular chiral liquid crystalline complex was later obtained [12] by the interaction of 4,4′-bipyridyl with 4-s-2-methylbutoxy benzoic acid; neither of the two complements of the complex was mesomorphic. According to their phase diagram [12], mixtures containing from 0.1 to 0.5 mol fraction of 4,4′-bipyridyl were found to exhibit polymorphism. Via hydrogen bonding interaction between mesomorphic and/or non-mesomorphic complementary components, the rigid-rod segment is lengthened, and thus induces liquid crystalline behaviour that may not occur in the individual components. Such induced mesomorphic behaviour was attributed to the formation of an elongated hydrogen-bonded complex. Furthermore, it is well established that the induction of liquid crystalline character is associated with the strength of hydrogen bonds formed between the interacting components. This would accordingly be affected by the change of polarity and/or polarisability of both components, upon change in their terminal polar substitution.

We have previously reported [13] the preparation and characterisation of new liquid crystal materials based on supramolecular hydrogen-bonded complexes between 4-(4′-pyridylazophenyl)-4″-alkoxy benzoates (as proton acceptors) and 4-substituted benzoic acids (as the proton donors). The proton acceptors were designed in such a manner to combine an azo, ester, and pyridine moieties within the same molecule. In addition, the alkoxy group in the para position with respect to the ester group of the base component of the complex may lead, in one way or another, to an increase in electron density on the pyridine nitrogen, due to its powerful electron-donating efficiency, and consequently enhances the stability of the hydrogen bond.

---

*Corresponding author. Email: magdinaoum@yahoo.co.uk

ISSN 0267-8292 print/ISSN 1366-5855 online

DOI: 10.1080/02678291003681378
http://www.informaworld.com

In continuation of our previous study [13–15] on supramolecular hydrogen-bonded complexes, we here prepare a new group of pyridine-based derivatives that carry a lateral-methyl group, namely, 4-(4′-pyridylazo-3-methylphenyl)-4″-alkoxybenzoates (**I***8*–**I***16*), aiming to investigate the effect of lateral (CH_3) substitution on the stability of the mesophase and, accordingly, on the stability of the associates formed between these pyridine-based derivatives (**I***8*–**I***16*) and each of the five mesomorphic 4-alkoxybenzoic acids (**II***8*–**II***16*), and the six non-mesomorphic 4-substituted benzoic acids (**II**$_{a\text{-}f}$).

The introduction of the lateral methyl group, into position-3 of the central benzene ring of the pyridine-based component, **III**, represents an attempt to reduce the melting point of the previously investigated supramolecular complexes [13]. The methyl group was chosen on the basis of its mild polarity. Molecular formulae of compounds used in the present investigation are given in Scheme 1.

2. Experimental details

Chemicals were of pure grades and purchased from the following companies: Fluka, Buchs, Switzerland; MP Biomedicals, Inc., Illkirch, France; BDH, Poole, England; Aldrich, Wisconsin, USA; and E. Merck, Darmstadt, Germany.

The molecular formulae of the newly prepared pyridine-based derivatives (**I***n*) were confirmed via elemental analyses, nuclear magnetic resonance (NMR), and mass spectroscopy. The results were in agreement, within the permissible limits, with the proposed structures. Infrared absorption spectra were measured with a Perkin-Elmer B25 spectrophotometer, and ^{1}H-NMR spectra with a Varian EM 350L.

Calorimetric measurements were carried out using a PL-DSC of Polymer Laboratories, England. The instrument was calibrated for temperature, heat and heat flow according to the method recommended by Cammenga *et al.* [16]. Differential scanning calorimetry (DSC) measurements were carried out for small samples (2–3 mg) placed in sealed aluminium pans. All of the thermograms have been achieved at a heating rate of 10°C min^{-1} in an inert atmosphere of nitrogen gas (10 ml min^{-1}).

Transition temperatures were checked and type of mesophase identified for the newly prepared base derivatives (**I***n*), and their associates with the acids (**II***n* and **II**$_{a\text{-}f}$), using a standard polarised optical microscope

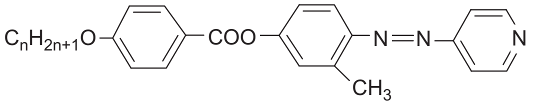

(**I***n*)

I*8*, $n = 8$, **I***10*, $n = 10$, **I***12*, $n = 12$, **I***14*, $n = 14$, **I***16*, $n = 15$

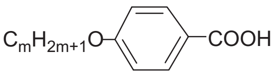

(**II***m*)

II*8*, $m = 8$, **II***10*, $m = 10$, **II***12*, $m = 12$, **II***14*, $m = 14$ and **II***16*, $m = 16$.

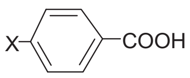

(**II**$_{a\text{-}f}$)

II$_a$, $X = CH_3O$, **II**$_b$, $X = CH_3$, **II**$_c$, $X = H$, **II**$_d$, $X = Cl$, **II**$_e$, $X = Br$, **II**$_f$, $X = CN$.

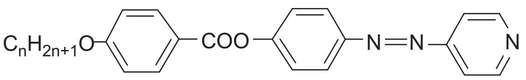

(**III***n*)

III*8*, $n = 8$, **III***10*, $n = 10$, **III***12*, $n = 12$, **III***14*, $n = 14$ and **III***16*, $n = 16$

Scheme 1. Molecular structures for compounds under investigation.

(POM) (Wild, Germany) attached to a home-made hot stage. The purity of samples prepared was checked with thin-layer chromatography (TLC) using TLC-sheets coated with silica gel (E. Merck), whereby spots were detected by a UV lamp. All components (**I***n*) were found to be TLC pure.

2.1 Preparation of materials

The pyridine-based azo dyes (**I***n*) were prepared according to Scheme 2.

The complexes (group **A** and **B**) were prepared according to Scheme 3.

2.1.1 Preparation of 4-(4′-pyridylazo)-3-methylphenol (A)

This was prepared according to the method described by Song *et al.* [17] from 4-aminopyridine and m-cresol. The yield of the crude product was 65 %, and melts at 232.6°C.

2.1.2 Preparation of 4-(4′-pyridylazo-3-methylphenyl)-4″-alkoxy benzoates (In)

This was prepared by the method described previously [13] for the preparation of the laterally neat analogues. The solids (approximately 50% yield) obtained were crystallised from ethanol and found to be TLC pure and to possess sharp melting temperatures as measured by DSC, and are given in Table 1. Elemental analyses were conducted for these newly prepared compounds and the results are included in Table 1.

2.1.3 Preparation of supramolecular complexes

For the preparation of the supramolecular complexes (**I/II**), binary mixtures of any two complementary components were prepared in a 1:1 molar ratio by melting the appropriate amounts of each component, stirring to give an intimate blend, and then cooling with stirring to room temperature.

For the construction of binary phase diagrams, mixtures of the two components were prepared to cover the whole range of composition. Transition temperatures obtained for all prepared blends, as measured by both DSC and POM, agreed within 2–3°C. In the phase diagrams, constructed by plotting transition temperatures versus mixture composition, the symbol ‘o’ denotes solid-mesophase, ‘□’ mesophase–isotropic transitions, ‘•’ mesophase–another mesophase, and ‘Δ’ eutectic temperature.

3. Results and discussion

3.1 Confirmation of molecular structure

The molecular formulae of the newly prepared pyridine-based homologues (**I***n*) were confirmed via

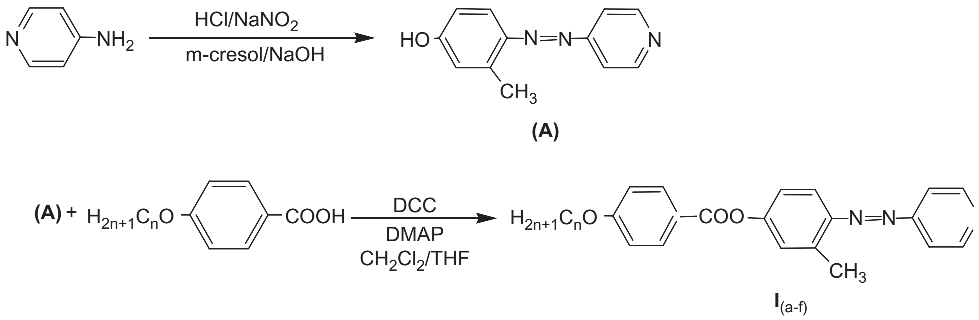

Scheme 2. Scheme for the preparation of compounds **I***n*.

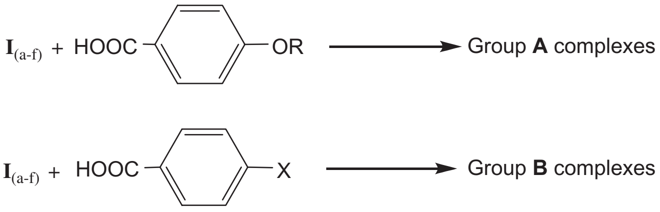

Scheme 3. Preparation of complexes of groups **A** and **B**.

Table 1. Transition temperatures (°C), transition enthalpies (kJ/mol), and elemental analyses of the pyridine-based azo dyes, **I***n*.

						Elemental Analyses Found (Calc.)		
Compound number	*n*	$T_{\text{Cr-I}}$	$\Delta H_{\text{Cr-I}}$	$^{\#}T_{\text{C-I}}$	$\Delta H_{\text{C-I}}$	% C	H %	N
I*8*	8	92.5	16.6	(79.7)	–0.2	72.65 (72.78)	7.19 (7.01)	9.32 (9.43)
I*10*	10	76.4	21	*77.4	0.4	73.99 (73.54)	7.06 (7.45)	8.90 (8.87)
I*12*	12	77.0	26.9	(76.2)	–0.2	74.02 (74.22)	7.89 (7.83)	8.70 (8.37)
I*14*	14	88.8	29.4	(77.3)	–0.2	74.61 (74.82)	8.05 (8.18)	8.34 (7.93)
I*16*	16	82.0	55	(75.7)	–0.7	75.99 (75.36)	8.61 (8.49)	7.60 (7.53)

Notes: Cr, denotes the solid phase,
I, denotes the isotropic phase,
*Enantiotropic transition from SmC to the isotropic phase,
$^{\#}$Parentheses denote the monotropic transition from SmC to the isotropic phase

elemental analyses, infrared (IR), NMR, and mass spectra. Elemental analyses (as given in Table 1) were in agreement, within permissible limits, with the proposed formulae. NMR data showed expected integrated aliphatic–aromatic ratios. Mass spectra indicated exact molecular masses for the whole molecular structures and expected fragmentation.

The nearly identical IR spectra observed for the five homologues (**I***n*) investigated revealed that the length of the alkoxy chain does not significantly affect the position of IR absorption bands; hence, for compound **I***10*, taken as a representative example, the C=O stretching absorption ($\upsilon_{C=O}$) appears at 1727 cm^{-1}, $\upsilon_{C=N}$ at 1608 cm^{-1}, $\upsilon_{C\text{-}O}$ at 1484 and 1273 cm^{-1}, symmetric and asymmetric υ_{CH_3} at 2849 and 2928 cm^{-1}, respectively. These results are consistent with the data reported before for the 4-CH_3O ($n = 1$) substituted homologue [18].

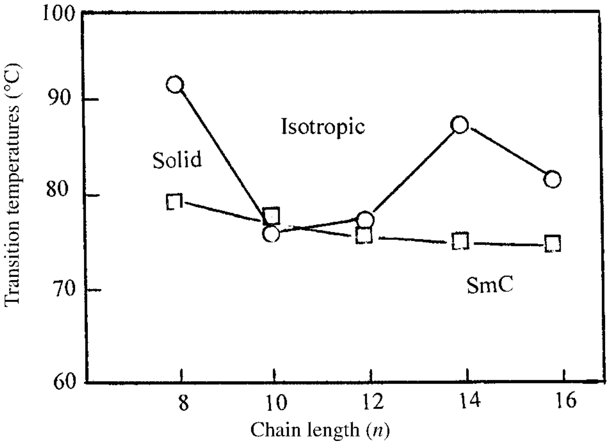

Figure 1. Effect of the alkoxy-chain length (*n*) on the mesophase behaviour of the pyridine-based derivatives **I***n*.

3.2 *Phase behaviour*

3.2.1 *Pyridine-based molecules*

Transition temperatures and transition enthalpies of the prepared pyridine-based derivatives (**I***n*) are given in Table 1. The data are represented graphically, as a function of the alkoxy-chain length (*n*) in Figure 1. As can be seen from Table 1 and Figure 1, except for the homologue **I***10*, all members of the series exhibit monotropic SmC mesophase. The melting temperatures (T_m) vary irregularly, as expected, with the increase of the alkoxy-chain length (*n*). Alternatively, the monotropic isotropic-to-SmC transition (T_C, □) decreases with the increase of *n*. The **I***10* homologue was found to exhibit a narrow range of an enantiotropic SmC phase, where it melts at 76.4°C and changes to the isotropic liquid at 77.4°C. On the other hand, cooling the isotropic melts recrystallise showing the SmC as the only mesophase observed.

Comparison of the data of the correspondingly substituted derivatives from groups **I** and **III** (see [13]) revealed that the introduction of a lateral methyl group into the central benzene ring resulted in a lowering of the melting point. These preliminary results have encouraged us to extend our investigation to constitute all possible supramolecular hydrogen-bonded complexes formed between the prepared, laterally methyl-substituted pyridine-based derivatives, **I***n*, and two series of 4-substituted benzoic acids. The

Table 2. Phase transition temperatures (°C) of the acids.

Acid	*n*	X	$T_{Cr\text{-}C}$	$T_{C\text{-}N}$	$T_{Cr\text{-}I}$	$T_{C\text{-}I}$	$T_{N\text{-}I}$
II8	8	-	101	108	-	-	147
II10	10	-	97	122	-	-	142
II12	12	-	95	129	-	-	137
II14	14	-	98	-	-	133	-
II16	16	-	85	-	-	132.5	-
$\mathbf{II}_a$	-	CH_3O	-	-	184	-	-
$\mathbf{II}_b$	-	CH_3	-	-	182	-	-
$\mathbf{II}_c$	-	H	-	-	122.1	-	-
$\mathbf{II}_d$	-	Cl	-	-	243	-	-
$\mathbf{II}_e$	-	Br	-	-	254.5	-	-
$\mathbf{II}_f$	-	CN	-	-	219	-	-
$\mathbf{II}_g$	-	NO_2	-	-	242	-	-

Notes: Cr, denotes the solid phase,
N, denotes the nematic phase,
I, denotes the isotropic phase.

first group of acid complements tested is the mesomorphic homologues of 4-alkoxy benzoic acids, **II***m*, in which *m* varies between 8 and 16 carbons. In the second series of acids, $\mathbf{II}_{a\text{-}f}$, all are non-mesomorphic and each is 4-substituted with a small compact polar group (X) that is changed between CH_3O, CH_3, Cl, Br, and CN, in addition to benzoic acid (X = H) itself.

Transition temperatures of the 4-substituted benzoic acids, as reported previously [13], are summarised in Table 2. As can be seen from the table, independent of the substituent X, none of the derivatives of the acids, $\mathbf{II}_{a\text{-}f}$, is mesomorphic, while all the 4-alkoxybenzoic acids are mesomorphic. The lower homologues, **II**8–**II**12 are polymorphic, possessing both nematic (N) and SmC mesophases, whereas the higher homologues, **II**14 and **II**16, are purely smectogenic, possessing SmC as the only mesophase. Such a difference in behaviour of the acids would definitely affect the mesophase behaviour of their complexes with the pyridine-based component in a variable manner.

3.2.2 Supramolecular hydrogen-bonded associates

*3.2.2.1 Group **A** complexes.* Generally, complementary components in a mixture employed for the formation of liquid crystal complexes may be either mesomorphic, non-mesomorphic, or both. Hydrogen bonding between the two components of the mixture leads to an elongation of the rigid segment of the individual components, as represented for group **A** complexes by Scheme 4.

Let us first investigate the binary phase behaviour of this system, in order to confirm complex formation between the pyridine-based derivatives and 4-alkoxy benzoic acids. As examples, we will construct the phase diagrams representing extremes in the length of the alkoxy chain on both sides of the complex, that is, mixtures of **I**8 with each of the acids **II**8 and **II**16 (Figure 2) and mixtures of **I**16 again with each of the same acids **II**8 and **II**16 (Figure 3). As can be seen from Figure 2, the nematic phase of the polymorphic acid **II**8 completely disappears upon the addition of about 40 mol% of **I**8. On the other hand, the enantiotropic SmC phase of either acid is retained in their binary mixtures up to the addition of 90 mol% of **I**8. In each case, complex formation in the solid as well as the mesophase is evidenced by the formation of two eutectic compositions, one preceding and the other following the 1:1 molar ratio; this is in addition to the enhanced stability of the SmC phase at this composition. Similar behaviour is observed (Figure 3) for the binary mixtures of the other homologue (**I**16) with the two acids **II**8 and **II**16, whereby both diagrams exhibit enhanced SmC stability for the 1:1 complexes in both systems.

Having been confirmed, all possible 1:1 complexes made from each of the homologues **I***n* with each of the acids **II***m* (group **A** complexes) were prepared and characterised for their phase behaviour by DSC, and the type of the mesophase was identified by POM. The results are collected in Table 3. Dependencies of the phase transition temperatures of the complexes

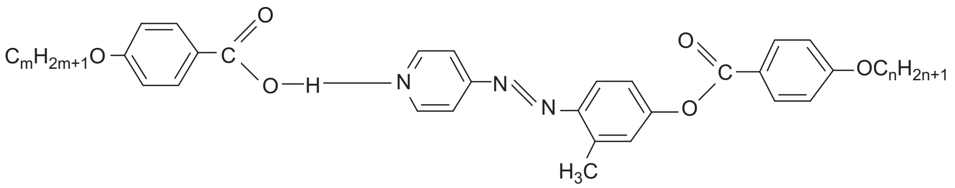

Scheme 4. Molecular structure of group **A** complexes.

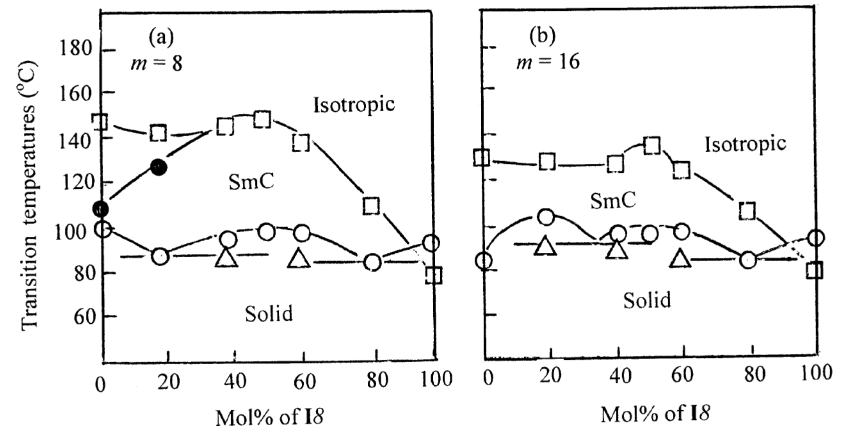

Figure 2. Binary phase diagrams of the pyridine-based derivative (**I***8*) with (a) octyloxy benzoic acid, and (b) hexadecyloxy benzoic acid.

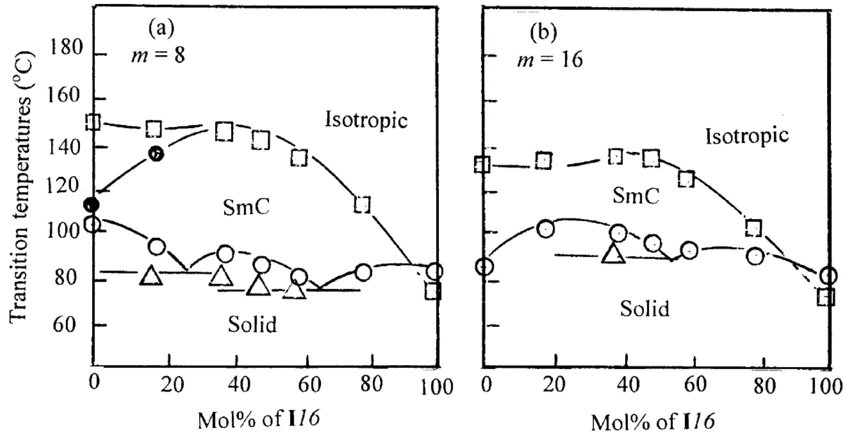

Figure 3. Binary phase diagrams of the pyridine-based derivative (**I***16*) with (a) octyloxy benzoic acid, and (b) hexadecyloxy benzoic acid.

prepared on the length of the terminal alkoxy-chain were represented graphically, once as a function of the pyridine-based alkoxy-chain length (*n*), and also against the acid alkoxy-chain length (*m*) in Figures 4 and 5, respectively. Both figures indicate that, irrespective of the length of the alkoxy chain on either side of the complex, SmC mesophase is the only mesophase observed in all of the complexes investigated. In either case, the stability of the SmC mesophase was found to decrease slightly with the increase of *n* or *m*. This behaviour can be attributed to the mesomorphic nature of the base component of the complex, where the SmC mesophase stability of the pyridine-based homologues was found to decrease with *n*, as shown in Figure 1.

*3.2.2.2 Group **B** complexes.* Generally, in hydrogen-bonded liquid crystals, phase behaviour is related to the strength of the hydrogen bond involved [19]. In the pyridine/acid complexes, association is primarily affected by the acidity of the proton donor, the acid, as well as the basicity of the pyridine derivative, the proton acceptor. In group **B** complexes (Scheme 5), the proton acceptor (**I***n*) is stabilised by the electron-donating character of the alkoxy group in the para position, whereas the acidity of the proton donor ($\mathbf{II}_{a\text{-}f}$) is affected to variable extents by the polarity of the substituent X attached to the para position with respect to the carboxyl group.

In order to obtain stoichiometric information on the binary mixtures of these types of complexes, two series of binary phase diagrams were constructed, using a varying mol% of **I***8* (or **I***16*) as proton acceptor, with each of the six acids ($\mathbf{II}_{a\text{-}f}$) individually as proton donors, and represented graphically in Figures 6 and 7, respectively. As can be seen from Figure 6, the homologue **I***8*, which possesses a monotropic SmC phase, enhances, in all of the non-mesomorphic 4-substituted acids, the

Table 3. Phase transition temperatures (°C) and transition enthalpies (kJ/mol) of the 1:1 supramolecular hydrogen-bonded complexes* of the systems $\mathbf{I}_{a\text{-}f}$/**II***n* (Group **A**).

System	*n*	*M*	$T_{Cr\text{-}C}$	$\Delta H_{Cr\text{-}C}$	$T_{C\text{-}I}$	$\Delta H_{C\text{-}I}$
I*8*/**II***8*	8	8	99.1	27.3	$T_{C\text{-}I}$	1.16
I*8*/**II***10*		10	95.4	52.9	149.9	1.54
I*8*/**II***12*		12	100.9	42.8	146.8	1.26
I*8*/**II***14*		14	92.9	70.4	142.5	2.28
I*8*/**II***16*		16	96.4	66.9	141.2	5.40
I*10*/**II***8*	10	8	100.2	44.2	137.2	1.81
I*10*/**II***10*		10	92.1	35.2	149.0	1.26
I*10*/**II***12*		12	97.1	38.2	143.3	1.30
I*10*/**II***14*		14	92.2	84.8	142.0	3.04
I*10*/**II***16*		16	95.2	68.2	134.7	1.75
I*12*/**II***8*	12	8	103.0	55.9	135.7	1.89
I*12*/**II***10*		10	94.6	66.2	142.8	1.96
I*12*/**II***12*		12	86.1	70.6	138.1	1.69
I*12*/**II***14*		14	85.8	65.7	137.3	1.05
I*12*/**II***16*		16	83.9	58.9	134.1	6.50
I*14*/**II***8*	14	8	80.8	47.0	130.7	1.30
I*14*/**II***10*		10	81.3	54.0	136.8	6.42
I*14*/**II***12*		12	86.8	72.4	134.7	8.04
I*14*/**II***14*		14	93.2	69.0	137.0	6.50
I*14*/**II***16*		16	96.4	93.2	132.2	8.58
I*16*/**II***8*	16	8	86.1	61.7	130.6	1.69
I*16*/**II***10*		10	81.2	53.8	139.0	1.40
I*16*/**II***12*		12	89.5	60.3	137.3	7.59
I*16*/**II***14*		14	86.0	59.7	135.8	7.46
I*16*/**II***16*		16	95.7	96.2	132.0	8.08

Notes: Cr, denotes the solid phase,
I, denotes the isotropic phase,
*Values given are for the 50 mol% compositions.

stability and mesomorphic ranges of the enantiotropic SmC mesophase. In their mixed solid phases, except with the 4-bromo substituted benzoic acid (Figure 6(e)), all other acids form solid complexes as evidenced by the two eutectic compositions. Figure 7, on the other hand, which shows the corresponding binary phase diagrams with the higher homologue **I***16*, revealed that, except with 4-methoxy benzoic acid that enhances the SmC mesophase of the complex, other acids proved to induce an enatiotropic SmC mesophase within a narrow range of composition with poor mesophase stability and mesomorphic range. This mesomorphic behaviour can be attributed to the difference in mesomorphic behaviour of the homologue **I***16*, compared with **I***8*.

In order to investigate the effect of the length of the alkoxy chain of the homologues **I***n* on the mesophase behaviour of their 1:1 complexes with 4-substituted benzoic acids (group **B** complexes), all possible complexes were prepared and their phase behaviour investigated by DSC and POM. The results (as given in Table 4) were plotted as a function of the alkoxy-chain length (*n*) in Figure 8. This shows that, except for the 4-chloro substituted complexes, **I***n*/$\mathbf{II}_d$, (Figure 8(d)), the SmC mesophase stability decreases with the increase of *n*. The melting point, as usual, changes irregularly with chain length. Unexpectedly, it was observed that the mesophase stability of the complexes **I***n*/$\mathbf{II}_d$ changes irregularly with the increase of *n*.

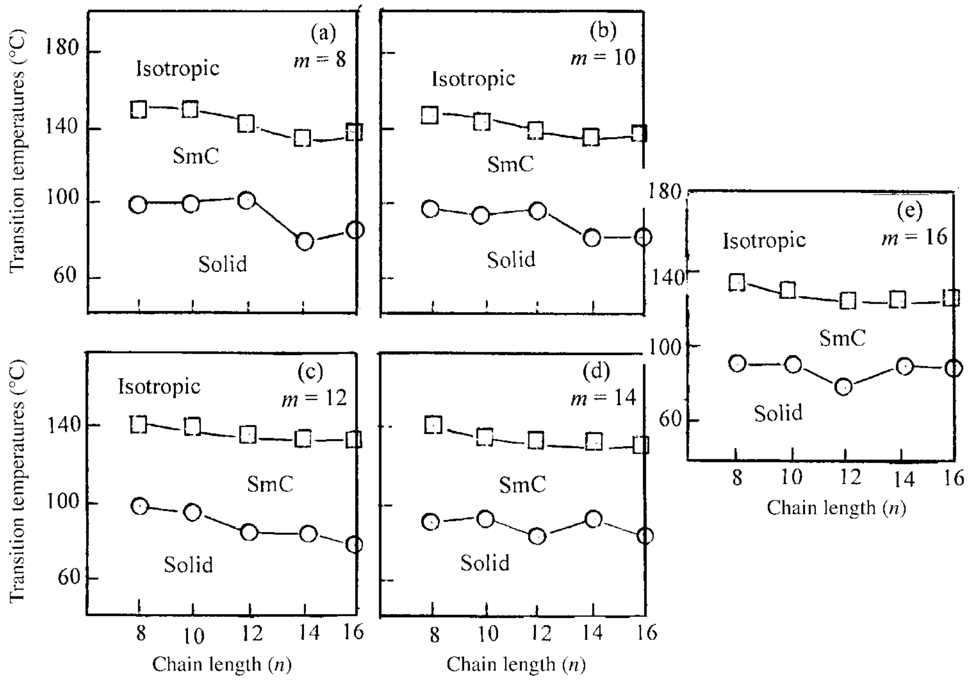

Figure 4. Effect of the pyridine-alkoxy chain length (*n*) on the mesophase behaviour of the 1:1 complexes of group **A**.

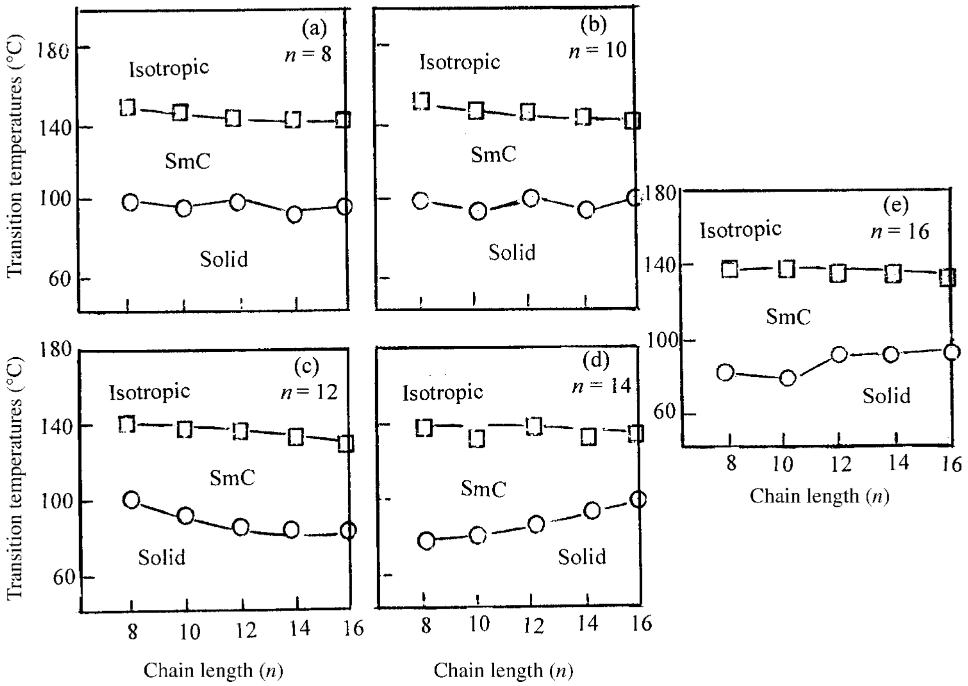

Figure 5. Effect of the acid-alkoxy chain length (*m*) on the mesophase behaviour of the 1:1 complexes of group **A**.

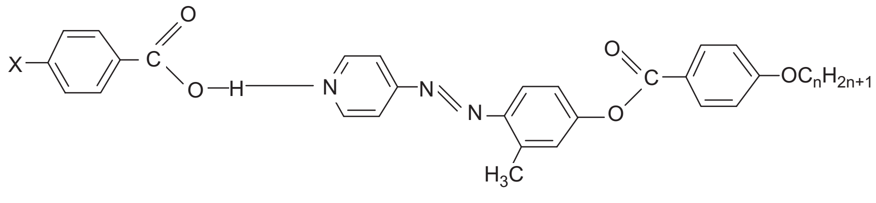

Group **B**

Scheme 5. Molecular structure of group **B** complexes.

As can be seen from Figures 6 and 7, the stability of the 1:1 complexes depends on the strength of H-bonding, which is facilitated by the electron-withdrawing substituent on the benzoic acid complement.

Referring to Tables 3 and 4, comparison between complexes of groups **A** and **B** revealed that while group **A** complexes are formed from acids bearing alkoxy groups of almost the same polarity, the acid complements in group **B** complexes bear substituents with varying polarity. So, the difference in the mesophase behaviour of group **A** complexes is mainly attributed to the variation in the alkoxy-chain length, while in group **B**, the variation of the mesophase behaviour of complexes is due to the difference in the polarity of the molecules.

3.3 Transition temperatures and polarisability anisotropy of the C_{ar}-X

The relationship between the stability of the mesophase, expressed as the clearing temperature, T_C, and the anisotropy of polarisability ($\Delta\alpha_X$) of bonds to the small compact terminal substituent (C_{ar}-X), was studied by van der Veen [20]. The relationship has the form:

$$T_C \alpha (\Delta\alpha_M + \Delta\alpha_X)^2 \qquad (1)$$

Where T_C is measured in Kelvin. Equation (1) can be put in the form [21]:

$$T_C^{1/2} \alpha (\Delta\alpha_M + \Delta\alpha_X) = a.\Delta\alpha_M + a.\Delta\alpha_X \qquad (2)$$

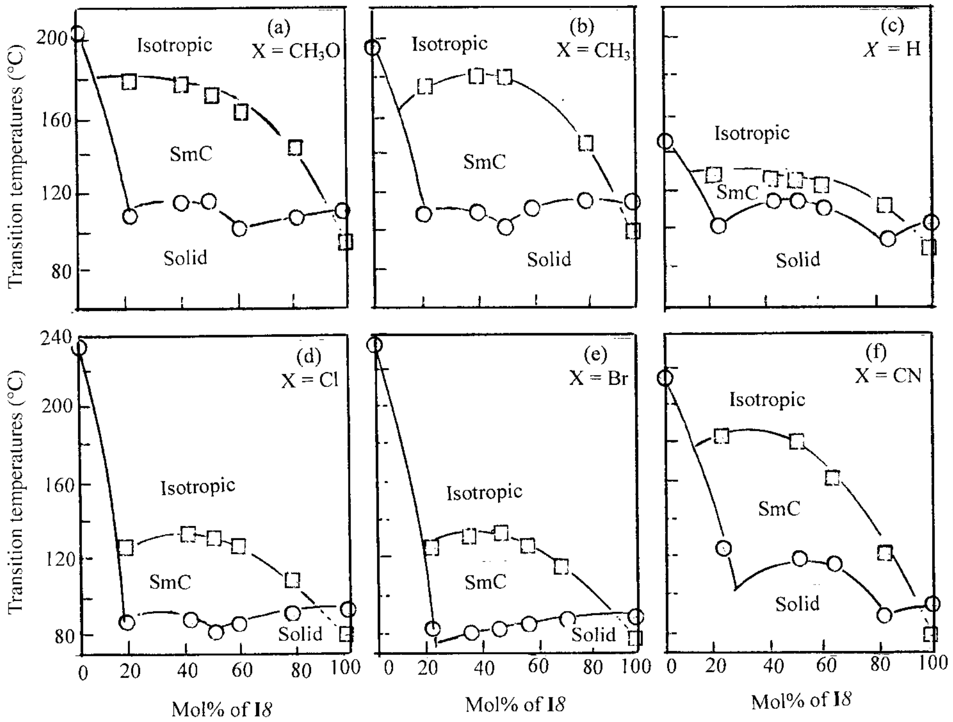

Figure 6. Binary phase diagrams of the pyridine-based derivative (**I***8*) with substituted benzoic acids, $\mathbf{II}_{a\text{-}f}$.

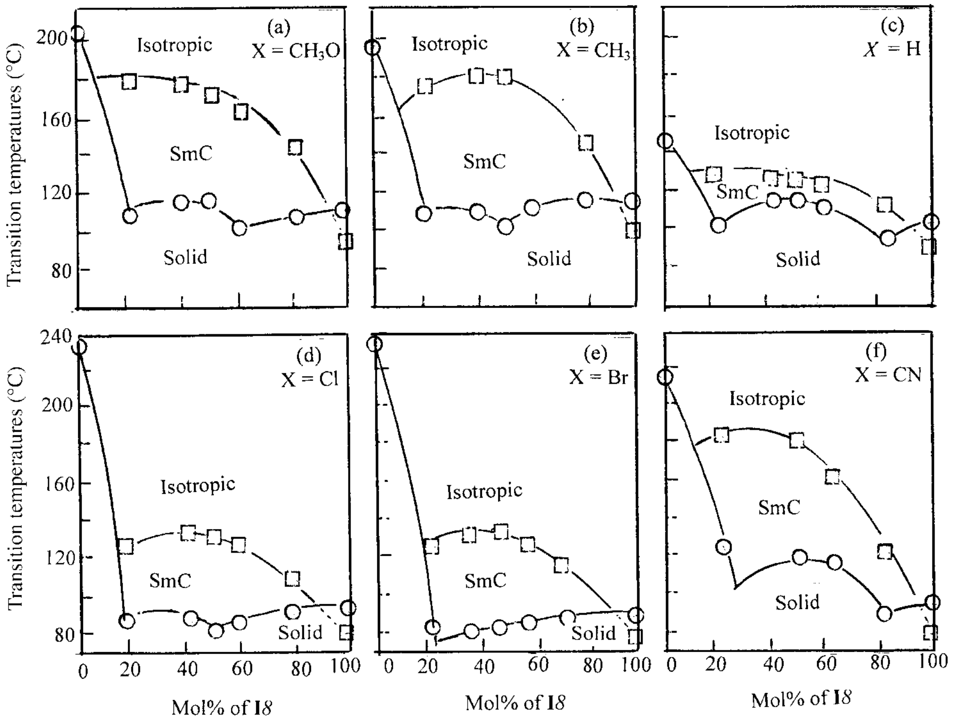

Figure 7. Binary phase diagrams of the pyridine-based derivative (**I***16*) with substituted benzoic acids, $\mathbf{II}_{a\text{-}f}$.

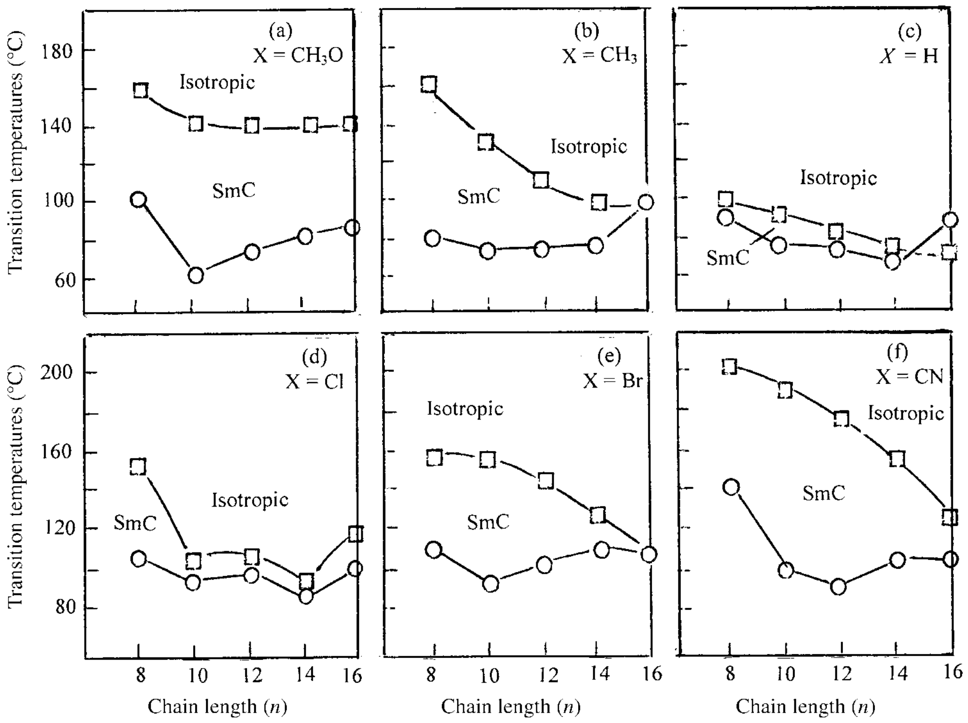

Figure 8. Effect of the pyridine-alkoxy chain length (n) on the mesophase behavior of the 1:1 complexes of group **B**.

The term $\Delta\alpha_M$ is the polarisability anisotropy of the whole molecular structure except the terminal substituent, X, and a is the proportionality constant. Thus, if, $T_C{}^{1/2}$ of any of our investigated hydrogen-bonded series of group **B,** bearing one and the same alkoxy group on the pyridine-based component n but of varying acid substitution **X**, is plotted against $\Delta\alpha_X$, a straight line is expected with a slope a and intercept equals a. $\Delta\alpha_M$, where a is the slope of the $\Delta\alpha_X$-dependency of $T_C{}^{1/2}$, and $\Delta\alpha_M$ is the polarisability anisotropy of the remainder of the molecular structure except the substituent (**X**). The $T_C{}^{1/2}$ values are plotted, individually, for each series bearing the same alkoxy group (n), as a function of the polarisability anisotropy $\Delta\alpha_X$ and depicted in Figure 9. Regression analyses data for the linear correlations drawn in Figure 9 are collected in Table 5. As can be seen from Figure 9, fairly linear dependencies were observed in the lower homologues of the base ($n = 8$) and goes far from being linear as n increases. This again indicates that increasing the base alkoxy chain does not favour mesophase formation.

4. Conclusions

The effect of introducing an alkoxy group of increasing chain length to the laterally methyl-substituted pyridine-based azo-dye derivatives of the type 4-(4′-pyridylazo-3-methylphenyl)-4″-alkoxy benzoates, **I***n*, on the possibility of formation, the stability and type of the mesophase observed for the prepared derivatives was investigated. Two groups of hydrogen-bonded supramolecular complexes were prepared and similarly investigated for their mesophase behaviour. In the first, group **A**, five homologues of the 4-alkoxybenzoic acids, **II***8*–**II***16*, were used and the 1:1 molar complex formation was confirmed by constructing the binary phase diagrams of two representative pyridine-based homologues (**I***8* and **I***16*) with two representative homologues of the acid. In the second group of complexes (group **B**) the acid complements, $\mathbf{II}_{a\text{-}f}$, were substituted, alternatively, with substituents of different polarity, namely, CH_3O, CH_3, Cl, Br, and CN, respectively. The study revealed the following:

(1) As evidenced from their binary phase diagrams, a 1:1 hydrogen-bonded complex is formed in the examples investigated that possesses the SmC mesophase as the only mesophase observed. Other 1:1 complexes of the other homologues proved to exhibit the SmC phase with reasonable range and stability.
(2) With respect to group **B** complexes, both electron-donating (CH_3O and CH_3) and electron-withdrawing (CN) substituents on the acid complement have

Table 4. Phase transition temperatures (°C) and transition enthalpies (kJ/mol) of the 1:1 supramolecular hydrogen-bonded complexes* of the systems **I***n*/**II**$_{a\text{-}g}$ (Group **B**).

System	*n*	X	$T_{Cr\text{-}C}$ (T_m)	$\Delta H_{Cr\text{-}C}$	$T_{C\text{-}I}$ (T_C)	$\Delta H_{C\text{-}I}$	$\sqrt{T_C}$ ($K^{1/2}$)
I*8*/**II**$_a$	8	CH_3O	99.0	41.9	156.0	0.25	20.7
I*8*/**II**$_b$		CH_3	81.1	46.7	162.9	0.24	20.8
I*8*/**II**$_c$		H	89.9	23.5	96.9	0.24	19.2
I*8*/**II**$_d$		Cl	85.4	39.5	134.3	1.01	20.1
I*8*/**II**$_e$		Br	87.8	43.5	135.7	8.38	20.2
I*8*/**II**$_f$		CN	120.9	25.8	183.2	3.47	21.3
I*8*/**II**$_g$		NO_2	60.6	43.2	139.1	2.35	20.3
I*10*/**II**$_a$	10	CH_3O	74.7	47.7	129.5	2.04	20.0
I*10*/**II**$_b$		CH_3	71.5	40.3	88.2	1.49	19.0
I*10*/**II**$_c$		H	73.4	43.2	82.7	0.26	18.8
I*10*/**II**$_d$		Cl	69.5	100.1	133.5	1.13	20.1
I*10*/**II**$_e$		Br	78.0	38.9	171.0	1.56	21.0
I*10*/**II**$_f$		CN	72.5	64.5	136.0	0.82	20.2
I*10*/**II**$_g$		NO_2	73.9	42.7	110.0	0.27	19.5
I*12*/**II**$_a$	12	CH_3O	73.7	57.9	79.5	0.26	18.7
I*12*/**II**$_b$		CH_3	76.5	53.7	85.3	0.55	18.9
I*12*/**II**$_c$		H	79.2	49.1	123.9	2.06	19.9
I*12*/**II**$_d$		Cl	69.2	57.3	155.0	0.94	20.6
I*12*/**II**$_e$		Br	81.6	53.0	140.0	1.42	20.3
I*12*/**II**$_f$		CN	75.3	56.2	97.6	0.84	19.2
I*12*/**II**$_g$		NO_2	65.6	64.0	71.6	1.08	18.5
I*14*/**II**$_a$	14	CH_3O	68.0	63.1	72.0	1.14	18.5
I*14*/**II**$_b$		CH_3	85.8	64.8	104.8	1.22	19.4
I*14*/**II**$_c$		H	83.6	48.4	136.7	2.55	20.2
I*14*/**II**$_d$		Cl	86.7	67.7	137.7	1.48	20.2
I*14*/**II**$_e$		Br	†99.0	57.7	-	-	-
I*14*/**II**$_f$		CN	82.3	65.6	67.5	0.57	18.4
I*14*/**II**$_g$		NO_2	80.8	66.0	96.6	0.90	19.2
I*16*/**II**$_a$	16	CH_3O	82.7	73.3	-	-	-
I*16*/**II**$_b$		CH_3	80.6	31.5	101.1	2.06	19.3
I*16*/**II**$_c$		H	99.0	41.9	156.0	0.25	20.7
I*16*/**II**$_d$		Cl	81.1	46.7	162.9	0.24	20.8
I*16*/**II**$_e$		Br	89.9	23.5	96.9	0.24	19.2
I*16*/**II**$_f$		CN	85.4	39.5	134.3	1.01	20.1
I*16*/**II**$_g$		NO_2	87.8	43.5	135.7	8.38	20.2

Notes: Cr, denotes the solid phase,
I, denotes the isotropic phase,
*Values given are for the 50 mol% compositions,
†Direct transition to isotropic.

shown to induce enatiotropic SmC phase in the 1:1 molar mixtures with the lower homologue (**I***8*) that covers a wider composition range, greater mesomorphic range and higher SmC stability compared with those of the higher **I***16* homologue. Comparison between the present results and those previously reported [13] for the laterally neat derivatives (**III**$_{a\text{–}e}$) revealed that methyl-lateral substitution into the central benzene ring of the pyridine-based compounds resulted in a lowering of melting point, but significantly affected the mesophase behaviour of their hydrogen-bonded associates with substituted benzoic acids.

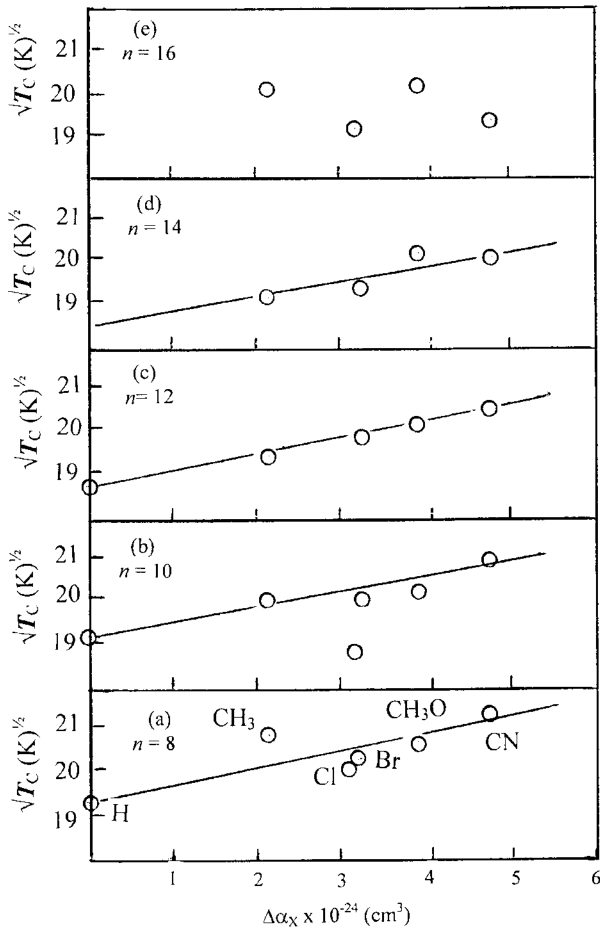

Figure 9. Dependence of the mesophase stability ($T_C^{1/2}$) of the investigated 1:1 adducts of group B on the polarisability anisotropy ($\Delta\sigma_X$) of the acid substituent (X).

Table 5. Regression analyses data for the van der Veen correlations for Group B complexes.

System	*n*	*X*	Slope ($\times 10^{23}$)	Intercept	$\Delta\alpha_M$ ($\times 10^{24}$)
I*8*/**II**	8	Varies	4.2	19.2	4.5
I*10*/**II**	10	Varies	3.5	19.2	5.4
I*12*/**II**	12	Varies	3.9	18.7	4.7
I*14*/**II**	14	Varies	3.6	18.5	5.1
I*16*/**II**	16	Varies	3.3	18.4	5.4

(3) The stability of the mesophase in group **B** complexes, expressed as the clearing temperature, was found to be greatly influenced by the nature of the substituent on the acid side of the new elongated mesogen. The unsubstituted and chloro-substituted benzoic acids furnish poor mesomorphic behaviour.

(4) Acceptable linear correlations, of $\sqrt{T_C}$ with the polarisability anisotropy of bonds to polar substituents attached to acid, were obtained that diminish as *n* increases.

References

[1] Paleos, C.M.; Tsiourvas, D. *Angew. Chem. Int. Ed. Engl.* **1995**, *34*, 1696–1711.

[2] Barmatov, E.B.; Pebalk, D.A.; Barmatov, M.V.; Shibaev, V.A. *Liq. Cryst.* **1997**, *23*, 447–451.

[3] Tian, Y.; Xu, X.; Zhoo, Y.; Li, T. *Liq. Cryst.* **1997**, *22*, 87–96.

[4] Letellier, P.; Ewing, D.F.; Goodby, I.W.; Haley, J.; Kelly, S.M.; Mackkenzie, G. *Liq. Cryst.* **1997**, *22*, 609–620.

[5] Sideratou, Z.; Tsiourvas, D.; Paleos, C.M.; Skoulios, A. *Liq. Cryst*. **1997**, *22*, 51–60.

[6] Raju, S.V.N.; Mule, S.A.; Rajan, C.R.; Ponratnam, S. *Ind. J. Chem*. **1997**, *36A*, 525.

[7] Kumar, P.A.; Srinivasulu, M.; Pisipati, V.G.K.M. *Liq. Cryst*. **1999**, *26*, 1339–1343.

[8] Swathi, P.; Kumar, P.A.; Pisipati, V.G.K.M. *Liq. Cryst*. **2000**, *27*, 665–669.

[9] Kato, T. In *Handbook of Liquid Crystals*; Demus, D., Goodby, J., Gray, G.W., Spiess, H.W., Vill, V., Eds.; Wiley-VCM: Weilheim, 1998; pp 969.

[10] Blunk, D.; Preafcke, K.; V. Vill. In *Handbook of Liquid Crystals*; Demus, D., Goodby, J., Gray, G.W., Spiess, H.W., Vill, V., Eds.; Wiley-VCM: Weilheim, 1998, pp 305.

[11] Kato, T.; Freachet, J.M.J. *J. Am. Chem. Soc*. **1989**, *111*, 8533–8534.

[12] Friot, B.; Boyd, D.; Willis, K.; Ungar, G.; Bruce, D.W. *Liq. Cryst*. **2000**, *27*, 605–611.

[13] Naoum, M.M.; Fahmi, A.A.; Alaasar, M.A. *Mol. Cryst. Liq. Cryst*. **2008**, *482*, 57–70.

[14] Naoum, M.M.; Fahmi, A.A.; Alaasar, M.A. *Mol. Cryst. Liq. Cryst*. **2008**, *487*, 74–91.

[15] Naoum, M.M.; Fahmi, A.A.; Alaasar, M.A. *Mol. Cryst. Liq. Cryst*. **2009**, *506*, 22–33.

[16] Cammenga, H.K.; Eysel, W.; Gmelin, E.; Hemmiger, W.; Hoehne, G.W.H.; Sagre, S.M. *Thermochim. Acta*. **1993**, *219*, 333–342.

[17] Song, X.; Li, J.; Zhang, S. *Liq. Cryst*. **2003**, *30*, 331–335.

[18] Naoum, M.M.; Fahmi, A.A.; Almllal, W.A. *Mol. Cryst. Liq. Cryst*. **2010**, *518*, 109–128.

[19] Bernhardt, H.; Weissflog, W.; Kresse, H. *Angew. Chem. Int. Ed. Engl*. **1996**, *35*, 874–876.

[20] van der Veen, J. *J. Phys. Colloq. C1* **1975**, *36*, 375–377.

[21] Naoum, M.M.; Saad, G.R.; Nessim, R.I.; Abdel Aziz, T.A. *Liq. Cryst*. **1998**, *25*, 73–83.